

Introducing the Condor Array Telescope. VI. Discovery of Extensive Ionized Gaseous Filaments of the Cosmic Web in the Direction of the M81 Group

KENNETH M. LANZETTA,¹ STEFAN GROMOLL,² MICHAEL M. SHARA,³ DAVID VALLS-GABAUD,⁴ FREDERICK M. WALTER,¹
AND JOHN K. WEBB⁵

¹*Department of Physics and Astronomy, Stony Brook University, Stony Brook, NY 11794-3800, USA*

²*Amazon Web Services, 410 Terry Ave. N, Seattle, WA 98109, USA*

³*Department of Astrophysics, American Museum of Natural History, Central Park West at 79th St., New York, NY 10024-5192, USA*

⁴*Observatoire de Paris, LERMA, CNRS, 61 Avenue de l'Observatoire, 75014 Paris, FRANCE*

⁵*Institute of Astronomy, University of Cambridge, Madingley Road, Cambridge CB3 9AL, UNITED KINGDOM*

(Received August 13, 2024; Accepted November 7, 2024)

Submitted to *Astrophysical Journal Letters*

ABSTRACT

We used the Condor Array Telescope to obtain deep imaging observations through luminance broad-band and He II, [O III], He I, H α , [N II], and [S II] narrow-band filters of an extended region of the M81 Group spanning $\approx 8 \times 8$ deg² on the sky centered near M81 and M82. Here we report aspects of these observations that are specifically related to (1) a remarkable filament known as the “Ursa Major Arc” that stretches ≈ 30 deg on the sky roughly in the direction of Ursa Major, (2) a “Giant Shell of Ionized Gas” that stretches ≈ 0.8 deg on the sky located ≈ 0.6 deg NW of M82, and (3) a remarkable network of ionized gaseous filaments revealed by the new Condor observations that appear to connect the arc, the shell, and various of the galaxies of the M81 Group and, by extension, the group itself. We measure flux ratios between the various ions to help to distinguish photoionized from shock-ionized gas, and we find that the flux ratios of the arc and shell are not indicative of shock ionization. This provides strong evidence against a previous interpretation of the arc as an interstellar shock produced by an unrecognized supernova. We suggest that all of these objects, including the arc, are associated with the M81 Group and are located at roughly the distance ≈ 3.6 Mpc of M81, that the arc is an intergalactic filament, and that the objects are associated with the low-redshift cosmic web.

Keywords: Galaxies (573), Galaxy groups (597), Galaxy interactions (600), Galaxy mergers (608), Galaxy photometry (611), Interacting galaxies (802), Low surface brightness galaxies (940), Galaxy tails (2125)

1. INTRODUCTION

Over the past several years, we have used the Condor Array Telescope (Lanzetta et al. 2023b) to obtain deep imaging observations through luminance broad-band and He II 468.6 nm, [O III] 500.7 nm, He I 587.5 nm, H α , [N II] 658.4 nm, and [S II] 671.6 nm narrow-band filters of an extended region of the M81 Group comprising 13 adjacent “Condor fields”¹ spanning $\approx 8 \times 8$ deg² on the sky centered near M81 and M82. Details of some of these observations are reported in a companion paper (Lanzetta et al. 2024, hereafter Paper V). These new Condor observations reveal extensive extended structures of ionized gas in the direction of the M81 Group, some of which are plausibly located within the Galaxy and some of which are plausibly located at the distance of M81.

Here we report aspects of these observations that are specifically related to (1) a remarkable filament known as the “Ursa Major Arc” (McCullough & Benjamin 2001; Bracco et al. 2020) that stretches ≈ 30 deg on the sky roughly in the direction of Ursa Major, (2) a “Giant Shell of Ionized Gas” (Lokhorst et al. 2022) that stretches ≈ 0.8 deg on the

¹ “Condor fields” are a set of fields with field centers that tile the entire sky with the Condor field of view, allowing for overlap.

sky located ≈ 0.6 deg NW of M82, and (3) a remarkable network of ionized gaseous filaments revealed by the new Condor observations that appear to connect the Ursa Major Arc, the Giant Shell of Ionized Gas, and various of the galaxies of the M81 Group and, by extension, the group itself. We suggest that this is a direct-imaging observation of the low-redshift cosmic web.

2. BACKGROUND AND CONTEXT

2.1. *Ursa Major Arc*

Over two decades ago, [McCullough & Benjamin \(2001\)](#) reported the discovery of faint $H\alpha$ emission from a long, straight, narrow filament extending ≈ 2.5 deg on the sky in the direction of Ursa Major. More recently, [Bracco et al. \(2020\)](#) reported observations obtained with GALEX ([Martin et al. 2005](#)) that show ultraviolet emission from this filament extending ≈ 30 deg on the sky, with a width ranging from less than one up to a few arcmin. This ‘‘Ursa Major Arc’’ has been interpreted variously as an interstellar trail of ionized gas produced by an unseen ionizing source ([McCullough & Benjamin 2001](#)) and as an interstellar shock produced by an unrecognized supernova ([Bracco et al. 2020](#)). The arc is clearly visible in the $H\alpha$ and [N II] mosaic difference images of Paper V, stretching across (and beyond) the entire images. It is notable that the Ursa Major Arc passes within only ≈ 45 arcmin of the center of M81.

2.2. *Giant Shell of Ionized Gas*

Recently, [Lokhorst et al. \(2022\)](#) reported the discovery of a shell of ionized gas that stretches ≈ 0.8 deg on the sky located ≈ 0.6 deg NW of M82 based on deep imaging observations through $H\alpha$ and [N II] 658.4 nm narrow-band filters of the vicinity of M81 and M82 obtained with the Dragonfly Spectral Line Mapper pathfinder. The authors argued that this ‘‘Giant Shell of Ionized Gas’’ is associated with M82 and the M81 Group rather than with the Galaxy. This interpretation is complicated by the low recession velocity of the group, which makes it difficult to unambiguously distinguish emission from the group from emission from the Galaxy, even with spectroscopic observations in hand. The authors nevertheless speculated that the shell might plausibly be ejected from M82 as a result of tidal interactions or the starburst activity of the galaxy or that the shell might plausibly be falling into M82 from the cosmic web in a way that is perhaps related to the superwind of the galaxy. The shell is clearly visible in the $H\alpha$ and [N II] mosaic difference images of Paper V, which reveal new details of the shell, as is discussed in Paper V and below.

3. CONDOR OBSERVATIONS AND DATA PROCESSING

The Condor observations of the M81 Group described in Paper V consist of deep imaging observations through luminance broad-band and He II, [O III], He I, $H\alpha$, [N II], and [S II] narrow-band filters of an extended region of the M81 Group comprising 13 adjacent Condor fields spanning $\approx 8 \times 8$ deg² on the sky centered near M81 and M82. The images were processed using the Condor data pipeline ([Lanzetta et al. 2023a,b](#)), and the various groups of coadded images were combined into seven mosaic images—one each obtained through the luminance and six narrow-band filters.

The M81 Group is located in a direction of significant Galactic cirrus, and starlight scattered from the cirrus dominates the diffuse light seen in both the broad- and narrow-band images. To at least a first approximation, any line emission is insignificant in comparison to continuum over the very wide bandpass of the luminance filter, so the luminance image roughly traces continuum while the narrow-band images trace line emission plus continuum. Accordingly, the luminance mosaic image was subtracted from the narrow-band mosaic images to yield difference mosaic images that trace more or less only line emission, and regions of the resulting mosaic images around stars contained in the Gaia DR3 catalog ([Gaia Collaboration et al. 2017, 2018, 2021; Gaia Collaboration 2022](#)) were masked at an isophotal limit, replacing the values of the masked pixels with the value of the median of nearby pixels. Details of this procedure are described in Paper V.

The net result of the observations and data processing described in Paper V is six continuum-subtracted, masked mosaic images through the He II, [O III], He I, $H\alpha$, [N II], and [S II] narrow-band filters of an extended region spanning $\approx 8 \times 8$ deg² on the sky centered near M81 and M82.

4. RESULTS

Selected portions of the mosaic difference images through the $H\alpha$ and [N II] filters are shown in Figure 1. In Figure 1, the left panel shows the $H\alpha$ image together with a schematic depiction of some of the features visible in the images. As is described in Paper V, this schematic depiction is not intended to be exhaustive or definitive but rather is intended only to label some of the possible features. In Figure 1, the middle panel shows a portion of the $H\alpha$ image, and

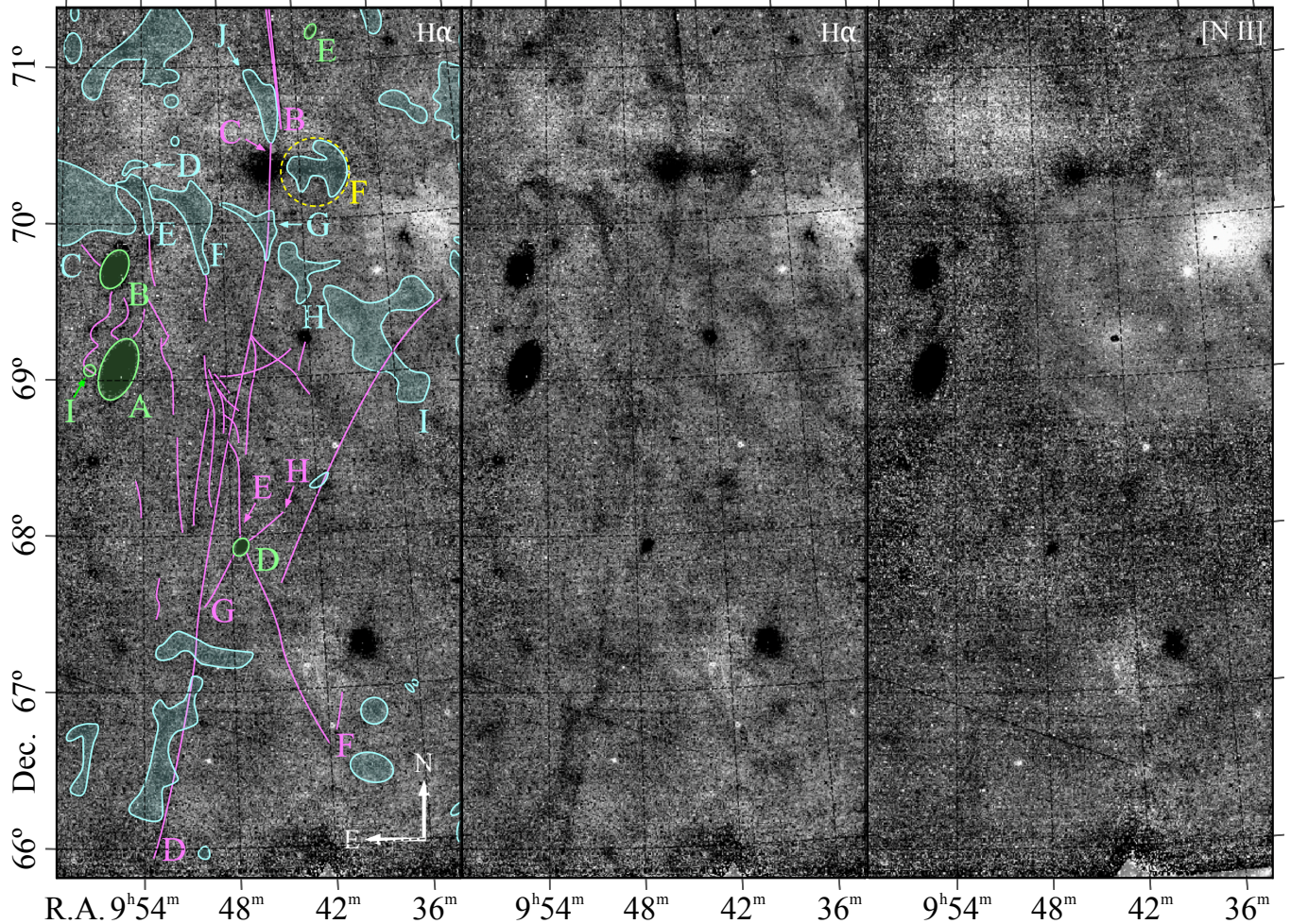


Figure 1. Selected portions of mosaic difference images through $H\alpha$ (left and middle panels) and $[N II]$ (right panel) filters formed by subtracting luminance broad-band image from narrow-band image and masking known stars. Left panel shows schematic depiction of some features visible in images. Galaxies are shown in light green, apparent clouds of gas are shown in light blue, filamentary or essentially one-dimensional structures are shown in pink, and an apparent or possible bubble or shell is shown as open yellow circle. M81, M82, and NGC 2976 are indicated in light green as galaxies A, B, and D, respectively. Clouds E and F are the Giant Shell of Ionized Gas, and filament BCD is the Ursa Major Arc. The bright unlabeled objects are stars. Each image spans $3.6 \times 5.5 \text{ deg}^2$, and for each image N is up and E is to left. Images are displayed block processed by 32×32 pixels, as described in Paper V.

the right panel show a portion of the $[N II]$ image. The schematic depiction of the left panel of Figure 1 indicates known galaxies of the M81 Group (shown in light green), apparent clouds of gas (shown in light blue), filamentary or essentially one-dimensional structures (shown in pink), and an apparent or possible bubble or shell (shown as open yellow circle). M81 and M82 are visible near the left-hand edges of the panels (as galaxies A and B, respectively), and NGC 2976 is visible below center of the panels (as galaxy D). We note the following:

First, the Ursa Major Arc is visible in $H\alpha$ and $[N II]$, stretching roughly N-S across (and beyond) the extent of the images. The character of the arc changes across the images in the sense that it is thicker and brighter toward the N and thinner and fainter toward the S. The arc appears to exhibit a discontinuity coincident with cloud J, and the southern segment of the arc appears to originate or terminate on cloud J.

Next, there is a remarkable network of criss-crossed ionized gaseous filaments that appear to intersect and overlap the Ursa Major Arc and various of the galaxies of the M81 Group. The filaments are visible in $H\alpha$, and some of the filaments are visible in $[N II]$. The widths of the filaments are typically ≈ 1 arcmin, i.e. comparable to the width of the Ursa Major Arc. The apparent epicenter of the network is located ≈ 0.9 deg SW of M81. Remarkably, there are

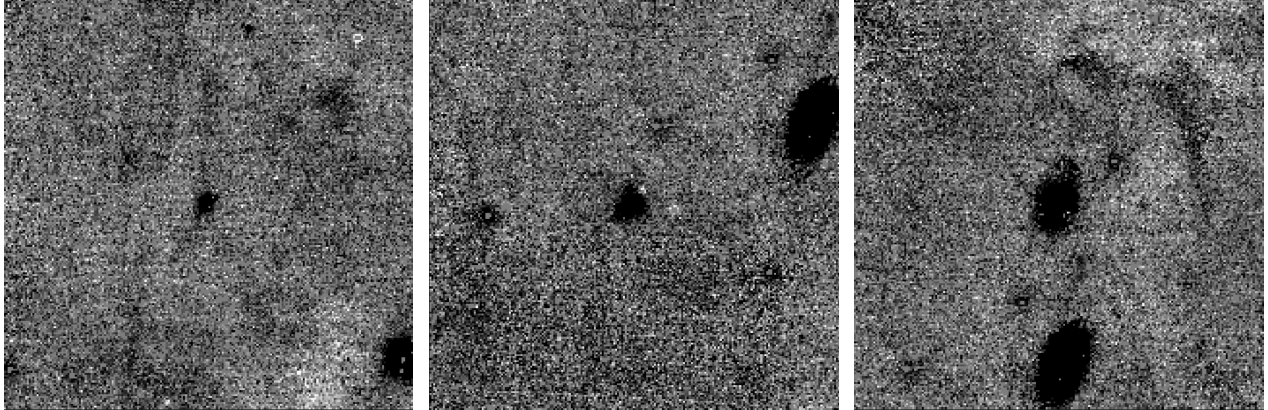


Figure 2. Expanded portions of mosaic difference image through $H\alpha$ filter centered on NGC 2976 (left panel), NGC 3077 (middle panel), and M82 (right panel). Each image spans $1.6 \times 1.6 \text{ deg}^2$, and for each image N is up and E is to left. Images are displayed block processed by 32×32 pixels, as described in Paper V.

four filaments that appear to originate or terminate on NGC 2976: one at roughly 12 o'clock (designated as filament E) and others at roughly 2 o'clock (filament H), 5 o'clock (filament F), and 7 o'clock (filament G). Filaments E and G appear to intersect the Ursa Major Arc toward the E (east) of the galaxy. Further, there is one filament that appears to originate or terminate on NGC 3077 (which is off the left-hand edges of and so not shown in the panels of Figure 1) at roughly 8 o'clock, and there are at least three filaments that appear to originate or terminate on M82, including filaments at roughly 2, 4, and 10 o'clock. Expanded portions of the mosaic difference image through the $H\alpha$ filter centered on NGC 2976, NGC 3077, and M82 are shown in Figure 2, in which these various filaments are visible. It is notable that the Ursa Major Arc passes within only ≈ 10 arcmin of the center of NGC 2976. The middle and right panels of Figure 2 also show a filament located ≈ 15 arcmin N of NGC 3077 and M82 and running roughly in the direction SE to NW that does not appear to originate or terminate on any galaxy.

Finally, the Giant Shell of Ionized Gas is visible in $H\alpha$ and $[N \text{ II}]$. The shell is clearly comprised of at least two pieces: an eastern piece designated as cloud E, and a western piece designated as cloud F. Both pieces exhibit similar morphologies, with a shape that resembles a “comma.” Further, both pieces appear to exhibit thin filaments that extend toward the S. The filament of cloud E appears to connect to the filaments of the western side of M82, and the filament of cloud F appears to connect to the network of criss-crossed filaments further to the S. It is notable that the Ursa Major Arc passes within only ≈ 20 arcmin of the western-most edge of cloud F. There is another cloud designated as cloud G located immediately W of cloud F that exhibits a morphology similar to those of clouds E and F, with a shape that resembles a comma; this cloud is exactly coincident with the Ursa Major Arc, and we suggest that it comprises part of the shell. In fact, clouds E, F, and G appear to form part of a larger chain of clouds that runs roughly NE to SW and includes clouds H and I to the W and other clouds (which are not shown in Figure 1 but are shown in Figure 8 of Paper V) K, L, M, and C to the E, and we suggest that all of these clouds might comprise part of the shell. Another smaller cloud D (which is shown in Figure 1) may also be associated with this chain and with the shell. Cloud J, which as noted above is coincident with the apparent discontinuity of the Ursa Major Arc, exhibits a morphology similar to those of clouds E, F, and G, with a shape that resembles a comma. Indeed there are dozens of other clouds visible in $H\alpha$ distributed throughout the mosaic image, especially toward the N and NW of M81, some (or all) of which may (or may not) be associated with the shell. (Again these other clouds are not shown in Figure 1 but are shown in Figure 8 of Paper V.) Some details of the shell are visible in the right panel of Figure 2. The bubble or shell F may be associated with the shell or the arc (or both).

5. DISCUSSION

The results of § 4 appear to show a direct connection between the Ursa Major Arc, the Giant Shell of Ionized Gas, the network of criss-crossed ionized gaseous filaments, and various of the galaxies of the M81 Group, including most dramatically NGC 2976. This apparent connection seems to imply that (1) all of these objects, including the Ursa Major Arc, are associated with the M81 Group and are located at roughly the distance ≈ 3.6 Mpc of M81 (Freedman

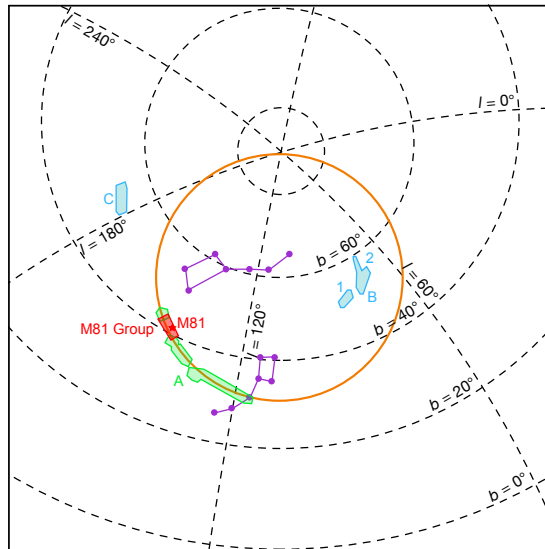


Figure 3. Stereographic projection of region of sky centered on purported center of circle along which arclets that comprise Ursa Major Arc appear to lie, based on Figure 2 of Bracco et al. (2020). Arclets that appear to lie along circumference of circle are indicated as feature A and shown in green, and arclets that do not lie along circle are indicated as features B1, B2, and C and shown in blue. Boundaries of Figure 1 are shown as red polygon, M81 is shown as red star, and approximate location of M81 Group is indicated. Circle of radius 29.28 deg centered on Galactic coordinates $(l, b) = (107^\circ.7, 60^\circ.0)$ is shown in orange. Grid shows Galactic coordinates, and Ursa Major and Ursa Minor are shown in purple.

et al. 1994) and (2) the Ursa Major Arc is an intergalactic filament rather than an interstellar trail of ionized gas or an interstellar shock. Here we consider additional evidence in support of this proposition.

5.1. Spatial Coincidences

The suggestion by Bracco et al. (2020) that the Ursa Major Arc is an interstellar shock produced by an unrecognized supernova is based primarily on their finding that the arc appears to be comprised of several piecewise-continuous arclets that roughly lie along ≈ 1 rad of the circumference of a circle of radius 29.28 ± 0.23 deg centered on Galactic coordinates $(l, b) = (107^\circ.7, 60^\circ.0)$. The authors also identified other arclets in the vicinity that do not lie along this circle. This is illustrated in Figure 3, which is based on Figure 2 of Bracco et al. (2020). Figure 3 shows a stereographic projection of a region of the sky centered on the purported center of the circle, where the arclets that appear to lie along the circumference of the circle are indicated as feature A and the arclets that do not lie along the circle are indicated as features B1, B2, and C; Figure 3 also indicates the boundaries of Figure 1, M81, and the approximate location of the M81 Group.

It is clear from Figure 3 that there is a remarkable spatial coincidence between the Ursa Major Arc and the M81 Group. This sets into broader context the previous statements that the Ursa Major Arc passes within ≈ 45 arcmin of M81, ≈ 10 arcmin of NGC 2976, and ≈ 20 arcmin western edge of cloud F and is exactly coincident with cloud G. While it is indeed striking that the arclets that comprise the Ursa Major Arc appear to roughly lie along the circumference of a circle, it is perhaps no less striking that the arc is essentially exactly aligned with one of the nearest galaxy groups beyond the Local Group, which itself appears to be criss-crossed by ionized gaseous filaments. Further, it appears from Figure 3 that it is at least plausible that, rather than tracing out the circumference of a circle, feature A is actually part of a larger structure that extends toward increasing Galactic latitude and longitude to encompass feature C (and perhaps even bends toward decreasing longitude to encompass features B1 and B2). We consider the remarkable spatial coincidence between the M81 Group and the Ursa Major Arc to provide strong circumstantial evidence in support of the proposition that the arc is an intergalactic filament associated with the M81 Group.

5.2. Ionization Mechanisms

One of our primary motivations for acquiring the Condor observations of the M81 Group was to exploit the diagnostic capabilities of deep imaging observations through [O III], $H\alpha$, [N II], and [S II] narrow-band filters to determine or constrain physical properties of ionized gas within the group. Measurements of flux ratios between these various ions

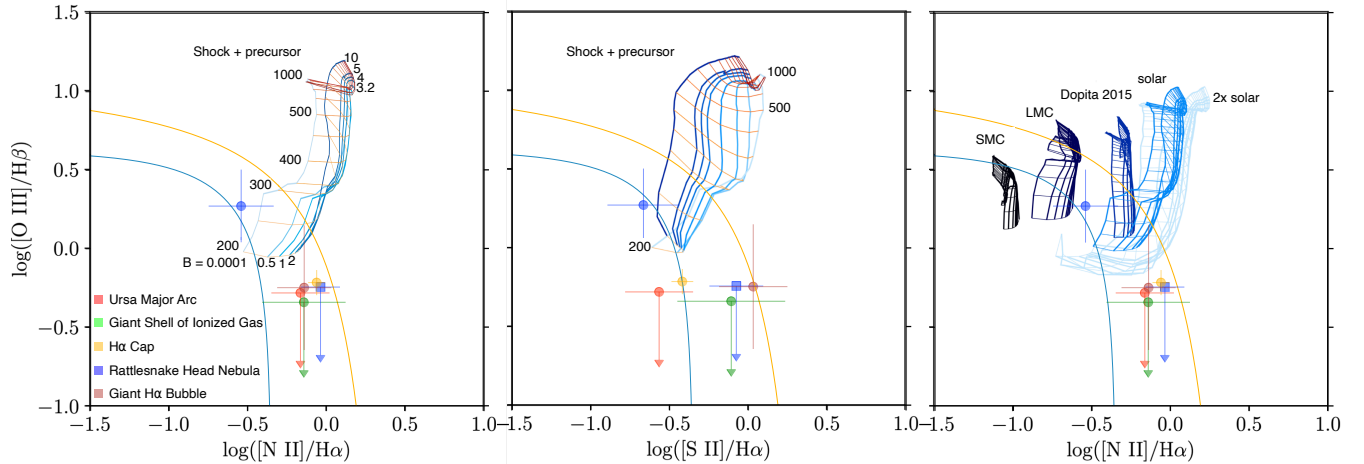


Figure 4. Measured and modeled flux ratios between ions of selected features. Measurements are of Ursa Major Arc (red), Giant Shell of Ionized Gas (green), H α Cap (orange), two portions of Rattlesnake Head Nebula (blue circle for SE portion and square for NW portion), and Giant H α Bubble (brown). Models are from MAPPINGS III “precursor plus shock” models of Allen et al. (2008) spanning a range of shock velocities, magnetic parameters, and abundances (see their figures 19, 21, and 23 for details). LMC and SMC abundance patterns are described by Russell & Dopita (1992). Blue and orange curves show empirical fiducial references set by Baldwin et al. (1981) and Kewley et al. (2001), respectively. The flux ratios provide strong evidence against the interpretation of the Ursa Major Arc as an interstellar shock produced by an unrecognized supernova.

can help to distinguish photoionized from shock-ionized gas (e.g. Baldwin et al. 1981; Veilleux & Osterbrock 1987), which bears on the nature and origin of the gas. The previous imaging observations of the Ursa Major Arc analyzed by Bracco et al. (2020) were carried out in only H α and continuum, and the previous imaging observations of the Giant Shell of Ionized Gas analyzed by Lokhorst et al. (2022) were carried out in only H α , [N II], and continuum (supplemented by spectroscopic observations of a portion of the shell), which limited the ability of these previous analyses to constrain the ionization mechanisms at play.

We measured flux ratios between ions of selected features in the images by the following procedure: First, we started with the 32×32 pix² block-processed mosaic images described in Paper V, because these images are insensitive to faint point sources (e.g. intergalactic H II regions). Next, we defined polygonal regions bounding the selected features, and we summed the energy fluxes of the various images within these regions to form the flux ratios. Next, we determined the median absolute deviations of the pixel-by-pixel ratios of the images within the regions to form robust measures of the spreads of the ratios. We applied this procedure to several of the features described in Paper V, including portions of (1) the Ursa Major Arc and (2) the Giant Shell of Ionized Gas and for comparison (3) the “H α Cap,” (4) the “Rattlesnake Head Nebula,” and (5) the “Giant H α Bubble.” The H α Cap is a well-known feature in the vicinity of M82 (Devine & Bally 1999; Lehnert et al. 1999), and the Rattlesnake Head Nebula and Giant H α Bubble are features discovered by the Condor observations presented in Paper V. The measurement of the Ursa Major Arc was made on the northernmost portion of the arc visible in Figure 8 of Paper V, where the arc is significantly brighter than it is over the extent of Figure 1. Two measurements of the Rattlesnake Head Nebula were made, one of the SE portion and one of the NW portion. The Condor observations cover H α but not H β , and so where necessary we adopted a value H α /H β = 2.86 appropriate for case-B photoionization (Osterbrock 1989); typical values of this ratio for shock-ionized gas are not too different from this (e.g. Gaskell & Ferland 1984), although this procedure does not account for possible extinction due to dust.

Results of the analysis are presented in Figure 4. Figure 4 shows the measurements described above overlaid with results of the MAPPINGS III “precursor plus shock” models of Allen et al. (2008) spanning a range of shock velocities, magnetic parameters, and abundances. In Figure 4, the left and right panels show log [O III]/H β versus log [N II]/H α , the middle panel shows log [O III]/H β versus log [S II]/H α , the left and middle panels are overlaid with models of solar abundances, and the right panel is overlaid with models of a range of abundances. The two measurements of the Rattlesnake Head Nebula are plotted separately in Figure 4, with portions to the SE and NW indicated by a blue circle and square, respectively, and indicate that the flux ratios vary significantly across the nebula.

It is clear from Figure 4 that, except for the SE portion of the Rattlesnake Head Nebula, the measured flux ratios of the various features are not indicative of shock ionization but rather are indicative of photoionization. In particular, the flux ratios of the Ursa Major Arc and the Giant Shell of Ionized Gas are similar to each other and to those of the H α Cap, the Giant H α Bubble, and the NW portion of the Rattlesnake Head Nebula. This result has two significant implications: (1) It provides strong evidence against the interpretation of the Ursa Major Arc as an interstellar shock produced by an unrecognized supernova. And (2) it suggests that the Ursa Major Arc and the Giant Shell of Ionized Gas are similar and may share a common ionization mechanism, which in turn bolsters the case that they share a common nature and origin. The measured flux ratios of the arc are also inconsistent with any of the radiative-shock models considered by Bracco et al. (2020) (which are based on results of Sutherland & Dopita 2017), which further undermines the interpretation as an interstellar shock. We consider the result that the flux ratios of the Ursa Major Arc are not indicative of shock ionization to provide strong evidence in support of the proposition that the arc is an intergalactic filament associated with the M81 Group.

The possibility that the Giant Shell of Ionized Gas is photoionized by the diffuse ultraviolet background radiation was considered in detail by Lokhorst et al. (2022), who found that the local background is insufficient to explain the observed H α surface brightness of the shell. If the arc, the shell, and the network of ionized filaments are indeed photoionized, then it is not clear what is the source of the ionizing radiation.

6. CONCLUSIONS

Based on (1) the direct connection between the Ursa Major Arc, the Giant Shell of Ionized Gas, the network of criss-crossed ionized gaseous filaments, and various of the galaxies of the M81 Group, (2) the remarkable spatial coincidence between the M81 Group and the Ursa Major Arc, and (3) the result that the flux ratios of the Ursa Major Arc are not indicative of shock ionization, we suggest that all of these objects are associated with the M81 Group and are located at roughly the distance ≈ 3.6 Mpc of M81 (Freedman et al. 1994), that the Ursa Major Arc is an intergalactic filament, and that objects are associated with the low-redshift cosmic web. We suggest that this is a direct-imaging observation of the low-redshift cosmic web.

If the Ursa Major Arc is indeed an intergalactic filament at the distance of the M81 Group, then its angular extent of ≈ 30 deg corresponds to a length of ≈ 1.9 Mpc, and its thickness, which ranges from ≈ 1 to 10 arcmin, corresponds to a width of ≈ 1 to 10 kpc. This seems thinner than might be expected for cosmic filaments but is consistent with the thinnest filaments seen in simulations of Ly α emission from the high-redshift cosmic web (e.g. Elias et al. 2020), and perhaps only the highest-surface-brightness portions of the filaments are visible. It is striking that the arc and the shell are of comparable surface brightness, with both exhibiting a maximum surface brightness of $\approx 7 \times 10^{-18}$ erg s cm $^{-2}$ arcsec $^{-2}$ or (≈ 1 Ry) and a typical surface brightness of $\approx 2.0 \times 10^{-18}$ erg s cm $^{-2}$ arcsec $^{-2}$ (or ≈ 0.3 Ry), at least over the extent of the observations presented here. Future efforts might seek to analyze spatially-resolved images of the various flux ratios using higher-signal-to-noise ratio images.

This material is based upon work supported by the National Science Foundation under Grants 1910001, 2107954, 2108234, 2407763, and 2407764. We gratefully acknowledge the staff of Dark Sky New Mexico, including Diana Hensley and Michael Hensley, for their superb logistical and technical support. KML acknowledges an enjoyable and productive visit to the Observatory of Paris, where much of this manuscript was written. The authors thank the anonymous referee for very valuable comments.

Software: astroalign (Beroiz et al. 2020), astropy (Astropy Collaboration et al. 2013, 2018), django (Django Software Foundation 2019), Docker (Merkel 2014), DrizzlePac (Gonzaga et al. 2012), NoiseChisel (Akhlaghi & Ichikawa 2015; Akhlaghi 2019), numba (Lam et al. 2015), numpy (Harris et al. 2020), photutils (Bradley et al. 2020), scipy (Virtanen et al. 2020), SExtractor (Bertin & Arnouts 1996)

REFERENCES

- Akhlaghi, M. 2019, arXiv e-prints, arXiv:1909.11230.
<https://arxiv.org/abs/1909.11230>
- Akhlaghi, M., & Ichikawa, T. 2015, ApJS, 220, 1,
 doi: 10.1088/0067-0049/220/1/1
- Allen, M. G., Groves, B. A., Dopita, M. A., Sutherland, R. S., & Kewley, L. J. 2008, ApJS, 178, 20,
 doi: 10.1086/589652

- Astropy Collaboration, Robitaille, T. P., Tollerud, E. J., et al. 2013, *A&A*, 558, A33, doi: [10.1051/0004-6361/201322068](https://doi.org/10.1051/0004-6361/201322068)
- Astropy Collaboration, Price-Whelan, A. M., Sipőcz, B. M., et al. 2018, *AJ*, 156, 123, doi: [10.3847/1538-3881/aabc4f](https://doi.org/10.3847/1538-3881/aabc4f)
- Baldwin, J. A., Phillips, M. M., & Terlevich, R. 1981, *PASP*, 93, 5, doi: [10.1086/130766](https://doi.org/10.1086/130766)
- Beroiz, M., Cabral, J., & Sanchez, B. 2020, *Astronomy and Computing*, 32, 100384, doi: <https://doi.org/10.1016/j.ascom.2020.100384>
- Bertin, E., & Arnouts, S. 1996, *A&AS*, 117, 393, doi: [10.1051/aas:1996164](https://doi.org/10.1051/aas:1996164)
- Bracco, A., Benjamin, R. A., Alves, M. I. R., et al. 2020, *A&A*, 636, L8, doi: [10.1051/0004-6361/202037975](https://doi.org/10.1051/0004-6361/202037975)
- Bradley, L., Sipőcz, B., Robitaille, T., et al. 2020, *astropy/photutils: 1.0.0*, Zenodo, doi: [10.5281/zenodo.4044744](https://doi.org/10.5281/zenodo.4044744), <https://doi.org/10.5281/zenodo.4044744>
- Devine, D., & Bally, J. 1999, *ApJ*, 510, 197, doi: [10.1086/306582](https://doi.org/10.1086/306582)
- Django Software Foundation. 2019, *Django*, 2.2.1. <https://djangoproject.com>
- Elias, L. M., Genel, S., Sternberg, A., et al. 2020, *MNRAS*, 494, 5439, doi: [10.1093/mnras/staa1059](https://doi.org/10.1093/mnras/staa1059)
- Freedman, W. L., Hughes, S. M., Madore, B. F., et al. 1994, *ApJ*, 427, 628, doi: [10.1086/174172](https://doi.org/10.1086/174172)
- Gaia Collaboration. 2022, *VizieR Online Data Catalog*, I/355
- Gaia Collaboration, Clementini, G., Eyer, L., et al. 2017, *A&A*, 605, A79, doi: [10.1051/0004-6361/201629925](https://doi.org/10.1051/0004-6361/201629925)
- Gaia Collaboration, Brown, A. G. A., Vallenari, A., et al. 2018, *A&A*, 616, A1, doi: [10.1051/0004-6361/201833051](https://doi.org/10.1051/0004-6361/201833051)
- . 2021, *A&A*, 649, A1, doi: [10.1051/0004-6361/202039657](https://doi.org/10.1051/0004-6361/202039657)
- Gaskell, C. M., & Ferland, G. J. 1984, *PASP*, 96, 393, doi: [10.1086/131352](https://doi.org/10.1086/131352)
- Gonzaga, S., Hack, W., Fruchter, A., & Mack, J. e. 2012, *The DrizzlePac Handbook*, STScI, Baltimore, MD
- Harris, C. R., Millman, K. J., van der Walt, S. J., et al. 2020, *Nature*, 585, 357, doi: [10.1038/s41586-020-2649-2](https://doi.org/10.1038/s41586-020-2649-2)
- Kewley, L. J., Dopita, M. A., Sutherland, R. S., Heisler, C. A., & Trevena, J. 2001, *ApJ*, 556, 121, doi: [10.1086/321545](https://doi.org/10.1086/321545)
- Lam, S. K., Pitrou, A., & Seibert, S. 2015, in *Proceedings of the Second Workshop on the LLVM Compiler Infrastructure in HPC*, 1–6
- Lanzetta, K. M., Gromoll, S., Shara, M. M., et al. 2023a, *PASP*, 135, 015002, doi: [10.1088/1538-3873/acae6](https://doi.org/10.1088/1538-3873/acae6)
- . 2024, *ApJS*
- . 2023b, *MNRAS*
- Lehnert, M. D., Heckman, T. M., & Weaver, K. A. 1999, *ApJ*, 523, 575, doi: [10.1086/307762](https://doi.org/10.1086/307762)
- Lokhorst, D., Abraham, R., Pasha, I., et al. 2022, *ApJ*, 927, 136, doi: [10.3847/1538-4357/ac50b6](https://doi.org/10.3847/1538-4357/ac50b6)
- Martin, D. C., Fanson, J., Schiminovich, D., et al. 2005, *The Astrophysical Journal*, 619, L1–L6, doi: [10.1086/426387](https://doi.org/10.1086/426387)
- McCullough, P. R., & Benjamin, R. A. 2001, *AJ*, 122, 1500, doi: [10.1086/322097](https://doi.org/10.1086/322097)
- Merkel, D. 2014, *Linux journal*, 2014, 2
- Osterbrock, D. E. 1989, *Astrophysics of gaseous nebulae and active galactic nuclei* (University Science Books)
- Russell, S. C., & Dopita, M. A. 1992, *ApJ*, 384, 508, doi: [10.1086/170893](https://doi.org/10.1086/170893)
- Sutherland, R. S., & Dopita, M. A. 2017, *ApJS*, 229, 34, doi: [10.3847/1538-4365/aa6541](https://doi.org/10.3847/1538-4365/aa6541)
- Veilleux, S., & Osterbrock, D. E. 1987, *ApJS*, 63, 295, doi: [10.1086/191166](https://doi.org/10.1086/191166)
- Virtanen, P., Gommers, R., Oliphant, T. E., et al. 2020, *Nature Methods*, 17, 261, doi: [10.1038/s41592-019-0686-2](https://doi.org/10.1038/s41592-019-0686-2)